Supporting Information

Enhanced photoelectrochemical water oxidation over a surface hydroxylated $BiVO_4$ photoanode: advantageous charge separation and water dissociation

Yaru Li[a], Fangxia Xie[a], Zijun Sun[a], Zhuobin Yu[b], Jianxin Liu[a], Xiaochao Zhang[a], Yawen Wang[a], Yunfang Wang[a], Rui Li[a,c,] *, Caimei Fan[a,] *

[a]*College of Chemical Engineering and Technology, Taiyuan University of Technology, Taiyuan 030024, PR China*

[b]*Instrumental Analysis Center, Taiyuan University of Technology, Taiyuan 030024, PR China*

[c]*College of Environmental Science and Engineering, Taiyuan University of Technology, Taiyuan 030024, PR China*

**Corresponding author*

Email address: lirui13233699182@163.com (R. Li); fancm@163.com (C.M. Fan)

Expressions used for the analysis [1]:

Applied bias photo-to-current efficiency (ABPE):

The applied bias photon-to-current efficiency of the different photoanodes was determined using the equation:

$$ABPE(\%) = \frac{J \times (1.23 - E_b)}{P_{total}} \times 100\% \qquad \text{(E1)}$$

where J is the photocurrent density (mA cm^{-2}) obtained from the LSV curve, P_{total} is the incident light intensity of the solar simulator (120 mW cm^{-2}), and E_b is the applied potential versus RHE (V).

Incident photon-to-current conversion efficiency (IPCE):

From the region of 420-700 nm excitation wavelengths at 1.23 V vs.RHE, the incident photon-to-current conversion efficiency (IPCE) was evaluated under chopped monochromator with a 300 W Xe lamp as the simulated light source (PLS-SXE 300+, Perfect Light, China) as:

$$IPCE(\%) = \frac{J \times 1240}{\lambda \times P_{light}} \times 100\% \qquad \text{(E2)}$$

where J is the photocurrent density (mA cm^{-2}) under illumination at a given wavelength, and P_{light} is the power density (mW cm^{-2}) of monochromatic light acquired at a given wavelength (λ).

Light harvesting efficiencies (LHE):

The efficiency of light harvesting may be represented as:

$$LHE(\lambda) = 1 - 10^{-A(\lambda)} \qquad \text{(E3)}$$

where $A^{(\lambda)}$ is the absorbance at specific wavelength λ.

The bulk charge separation (η_{sep}) and surface charge injection efficiency (η_{inj}):

The measured water splitting photocurrent can be expressed as:

$$J_{PEC} = J_{abs} \bullet \eta_{sep} \bullet \eta_{inj} \qquad \text{(E4)}$$

J_{abs} is the photocurrent density (mA cm^{-2}) if all absorbed photons can be converted to current. The following equation can be used to estimate J_{abs}:

$$J_{abs} = J_{max} \bullet LHE \qquad \text{(E5)}$$

where LHE is light harvesting efficiency, and J_{max} is maximum photocurrent density (mA cm^{-2}) achievable assuming 100% IPCE for photons with energy ≥E_g.

Surface recombination of the charge carriers may be entirely inhibited in the presence of hole scavenger Na_2SO_3, without affecting charge separation in the electrode bulk (η_{inj}=100%). As a result, the η_{sep} and η_{inj} may be computed using the formulae below:

$$\eta_{sep} = \frac{J_{Na_2SO_3}}{J_{abs}} \qquad \text{(E6)}$$

$$\eta_{inj} = \frac{J_{Na_2SO_4}}{J_{Na_2SO_3}} \qquad \text{(E7)}$$

where J_{Na2SO3} is the photocurrent density (mA cm^{-2}) measured in the electrolyte of 0.1 M Na_2SO_4 with 0.1 M Na_2SO_3, and J_{Na2SO4} is the photocurrent density (mA cm^{-2}) obtained in 0.1 M Na_2SO_4 electrolyte.

Supplementary figures and tables:

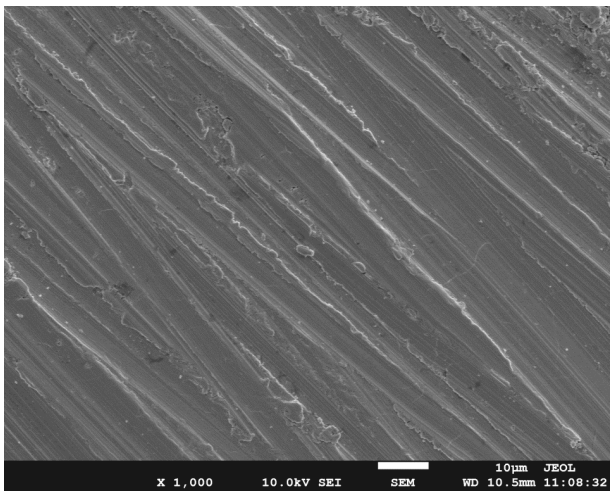

Fig. S1 SEM image of the metal Bi substrate.

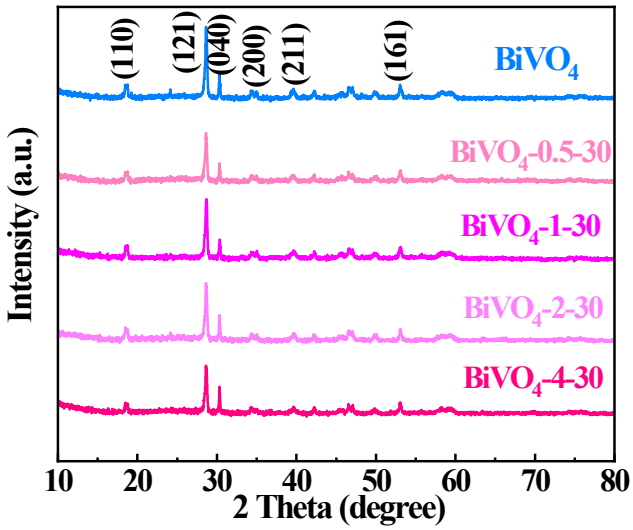

Fig. S2 XRD patterns of the prepared samples treated with different concentration NaOH solutions.

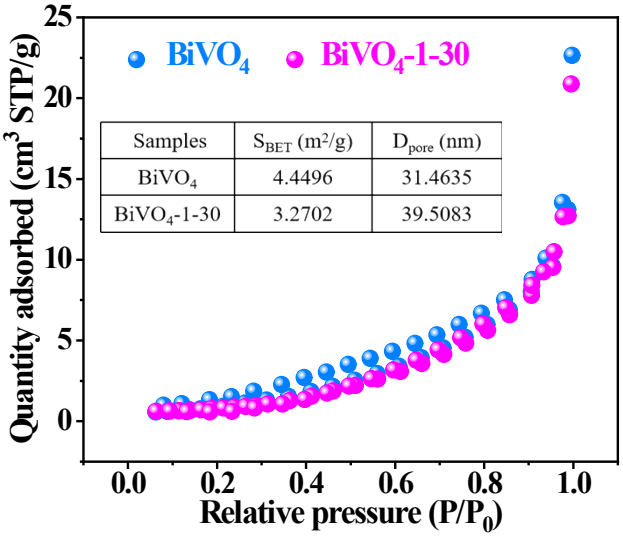

Fig. S3 The N_2 adsorption-desorption isotherms and the inset of the related parameters of bare $BiVO_4$ and $BiVO_4$-1-30 photoanodes.

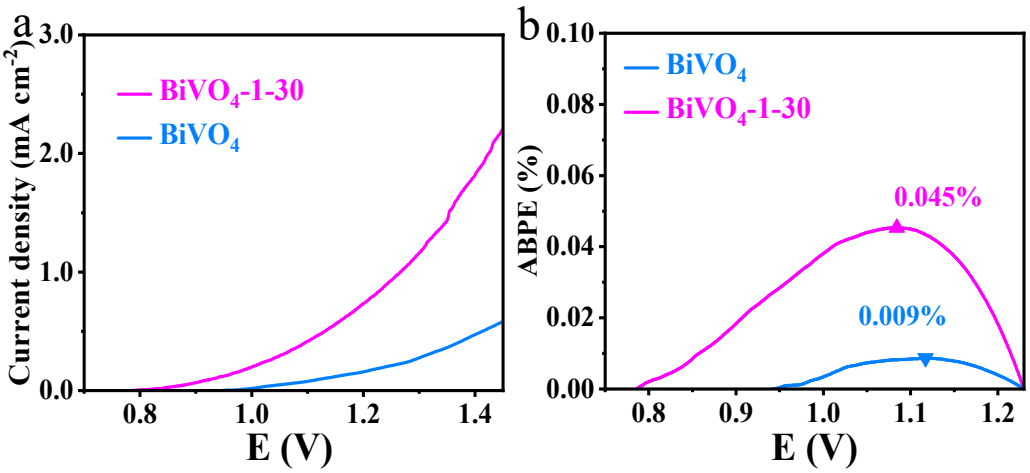

Fig. S4 (a) LSV and (b) ABPE curves performed in the two-electrode configuration, in which the Pt wire is as counter electrode and the bare $BiVO_4$ and $BiVO_4$-1-30 photoanodes are as working electrode, respectively.

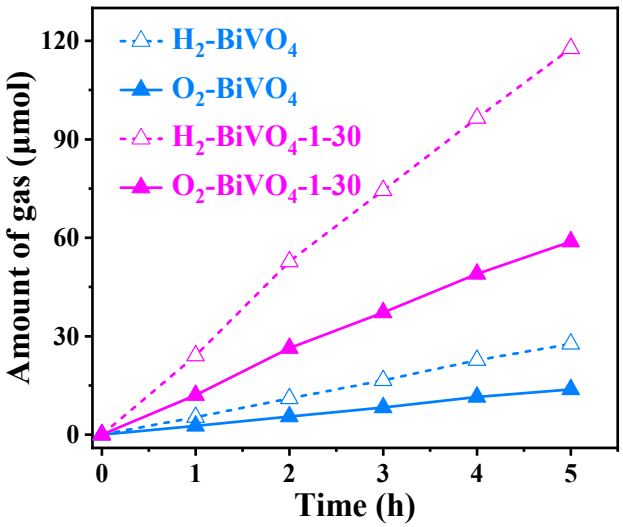

Fig. S5 The amount of H_2 and O_2 gases generated from the bare $BiVO_4$ and $BiVO_4$-1-30 photoanodes at 1.23 V vs. RHE during 5 hours.

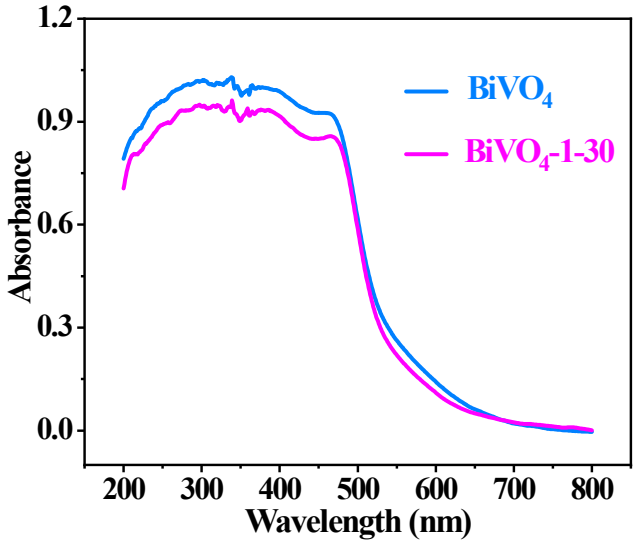

Fig. S6 The UV-vis diffuse reflectance spectra (DRS) of bare $BiVO_4$ and $BiVO_4$-1-30 photoanodes.

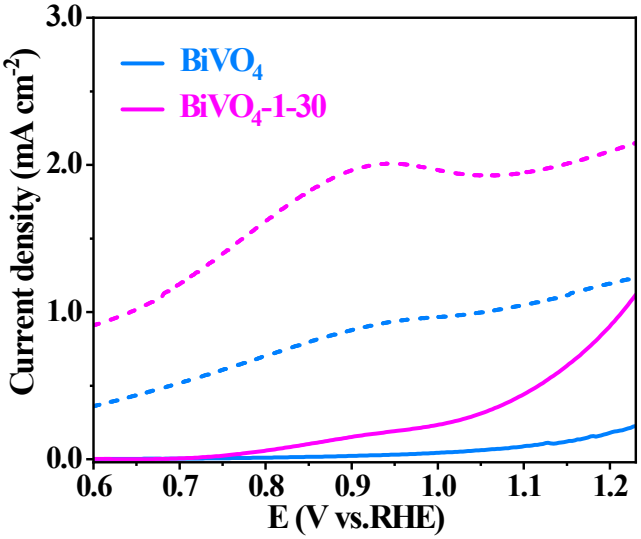

Fig. S7 LSV curves for sulfite oxidation and H_2O oxidation measured in the electrolytes of 0.1 M Na_2SO_4 containing 0.1 M Na_2SO_3 (broken lines) and without Na_2SO_3 (solid lines) of bare $BiVO_4$ and $BiVO_4$-1-30 photoanodes.

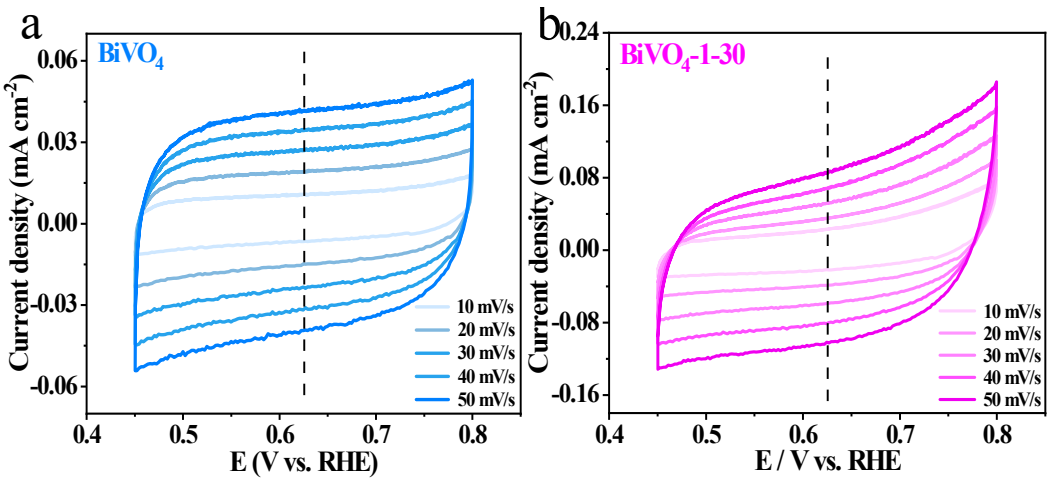

Fig. S8 Cyclic voltammograms for (a) bare $BiVO_4$, (b) $BiVO_4$-1-30 photoanodes at different scan rates (10, 20, 30, 40 and 50 mV s^{-1}).

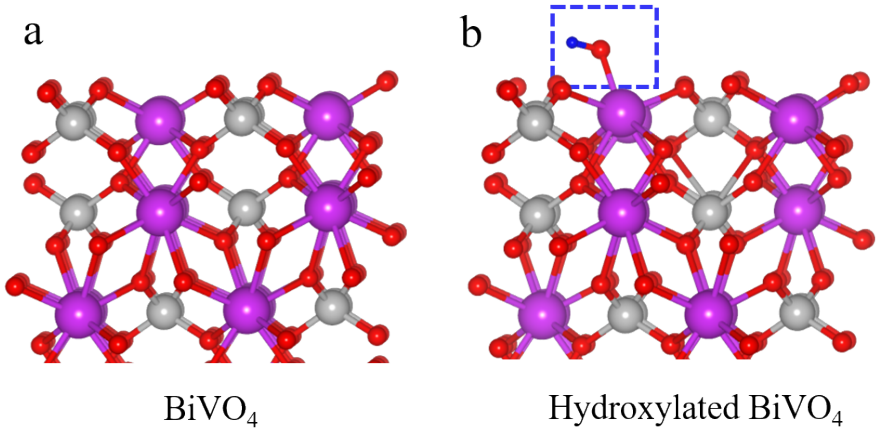

Fig. S9 Theoretical models of (a) bare $BiVO_4$ and (b) hydroxylated $BiVO_4$.

Table S1 The PEC water oxidation properties and preparation methods of the reported $BiVO_4$-based photoanodes.

Catalysts	Fabrication method	Electrolyte	Performance	References
$BiVO_4$	in-situ hydrothermal	0.1 M Na_2SO_4	J=0.24 mA cm^{-2}, η_{sep}=16.45%, η_{inj}=19.22% at 1.23 V_{RHE}, ABPE=0.014% at 1.05 V_{RHE} and IPCE=3.69%	This work
Surface hydroxylated $BiVO_4$	in-situ hydrothermal and immersion		J=1.14 mA cm^{-2}, η_{sep}=28.7%, η_{inj}=53.16% at 1.23 V_{RHE}, ABPE=0.049% at 1.09 V_{RHE} and IPCE=16%	
$BiVO_4$	repeated spin coating/calcination procedure and anneal	0.1 M Na_2SO_4	J=0.18 mA cm^{-2} at 1.23 V_{RHE}	2
Ag-$BiVO_4$/$BiFeO_3$			J=0.72 mA cm^{-2} at 1.23 V_{RHE}	
$BiVO_4$	chemical solution deposition and hydrothermal	0.5 M Na_2SO_4	J=0.5 mA cm^{-2}, ABPE=0.074% at 0.312 V_{RHE} and IPCE=16.14%	3
$BiVO_4$/$CoNiO_2$			J=1.16 mA cm^{-2}, ABPE=0.163% at 0.312 V_{RHE} and IPCE=34.37%	
$BiVO_4$	electrodeposition and calcination	0.2 M Na_2SO_4	J=0.35 mA cm^{-2}, ABPE=0.028% at 0.9 V_{RHE} and IPCE=14.7%	4
α-FOOH/$BiVO_4$	electrodeposition, calcination and chemical bath deposition		J=2.64 mA cm^{-2}, ABPE=0.59% at 0.9 V_{RHE} and IPCE=62.7%	
$BiVO_4$	multistep electrodeposition and annealed	0.1 M PBS	J=0.18 mA cm^{-2}, η_{sep}=18.2%, η_{inj}＜10% at 1.23 V_{RHE}, ABPE=0.03% at 0.8 V_{RHE} and IPCE=62.7%	5
$BiVO_4$/SnO_2			J=0.56 mA cm^{-2}, ABPE=0.08% at 0.8 V_{RHE} and IPCE=62.7%	
$NiWO_4$/$BiVO_4$/SnO_2			J=0.93 mA cm^{-2}, η_{sep}=23%, η_{inj}=30% at 1.23 V_{RHE}, ABPE=0.21% at 0.8 V_{RHE} and IPCE=62.7%	
$BiVO_4$	electrodeposition and anneal transformation	0.5 M Na_2SO_4	J=0.47 mA cm^{-2}, η_{sep}=40%, η_{inj}=18% at 1.23 V_{RHE}, ABPE=0.11% at 1.03 V_{RHE} and IPCE=10%	6
$BiVO_4$/Bi_2S_3	high temperature ion exchange and anneal		J=0.92 mA cm^{-2}, η_{sep}=47%, η_{inj}=35% at 1.23 V_{RHE}, ABPE=0.21% at 1.07 V_{RHE} and IPCE=21%	
$BiVO_4$/Bi_2S_3/$NiCoO_2$	drop casting and anneal		J=2.58 mA cm-2, η_{sep}=54%, η_{inj}=80% at 1.23 V_{RHE}, ABPE=0.62% at 1.11 V_{RHE} and IPCE=42%	

Table S2 The reported typically surface hydroxylation methods.

Catalysts	**Fabracation method**	**Application field**	**References**
$BiVO_4$	post-synthetic NaOH immersion	photoelectrochemical water oxidation	This work
α-Fe_2O_3	ultrasonically treating in water	photoelectrochemical water oxidation	7
TiO_2/g-C_3N_4	plasma treating	photo-Fenton degradation of tetracycline	8
g-C_3N_4	high temperature heating with mixed NaOH	photocatalytic degradation of phenol	9
g-C_3N_4	ultrasonically treating in H_2O_2 solution	photocatalytic CO_2 reduction	10
Zn_2GeO_4	hydrothermally treating in NaOH solution	photocatalytic conversion of CO_2 into CH_4	11
polymeric carbon nitride	hydrothermal route in water	photocatalytic H_2 evolution	12
SiO_2/g-C_3N_4	heating reflux in H_2O_2 solution	photocatalytic degradation rate of rhodamine B	13

References

[1] X. Lv, X. Xiao, M. Cao, Y. Bu, C. Wang, M. Wang and Y. Shen, Appl. Surf. Sci., 2018, **439**, 1065-1071.

[2] T. Soltani and B. Lee, Sci. Total Environ., 2020, **736**, 138640.

[3] G. Fang, Z. Liu, C. Han, X. Ma, H. Lv, C. Huang, Z. Cheng, Z. Tong and P. Wang, Chem. Commun., 2020, **56**, 9158.

[4] W. Zhang, J. Ma, L. Xiong, H. Jiang and J. Tang, ACS Appl. Energy Mater., 2020, **3**, 5927-5936.

[5] M. Shaddad, P. Arunachalam, M. Hezam and A. Al-Mayouf, Catalysts, 2019, **9**, 879.

[6] S. Majumder, M. Gu and K. Kim, Appl. Surf. Sci., 2022, **574**, 151562.

[7] C. Tang, B. Sun, M. Li, J. Zhang, X. Fan, F. Gao, Y. Tong, L. Dong and Y. Li, J. Mater. Chem. A, 2019, **7**, 8050.

[8] Y. Li, Q. Zhang, Y. Lu, Z. Song, C. Wang, D. Li, X. Tang and X. Zhou, Ceram. Int., 2022, **48**, 1306-1313.

[9] J. Ma, C. Liang, H. Li, H. Xu, Y. Hua and C. Wang, Appl. Surf. Sci., 2021, **546**, 149085.

[10] I. Khan, X. Chu, I. Khan, H. Liu, W. Li, L. Bai and L. Jing, Mater. Res. Bull., 2020, **130**, 110926.

[11] S. Yan, J. Wang, Z. Zou and Dalton Trans., 2013, **42**, 12975.

[12] S. Yu, J. Li, Y. Zhang, M. Li, F. Dong, T. Zhang and H. Huang, Nano Energy, 2018, **50**, 383-392.

[13] S. Sun, C. Li, Z. Sun, J. Wang, X. Wang and H. Ding, Chem. Eng. J., 2021, **416**, 129107.